Disentangling molecular motions involved in the glass transition of a twist-bend nematic liquid crystal through dielectric studies

D. O. López, N. Sebastian, M. R. de la Fuente, J. C. Martínez-García, J. Salud et al.

Citation: J. Chem. Phys. **137**, 034502 (2012); doi: 10.1063/1.4733561
View online: http://dx.doi.org/10.1063/1.4733561
View Table of Contents: http://jcp.aip.org/resource/1/JCPSA6/v137/i3
Published by the American Institute of Physics.

Disentangling molecular motions involved in the glass transition of a twist-bend nematic liquid crystal through dielectric studies

D. O. López,[1,a)] N. Sebastian,[2] M. R. de la Fuente,[2] J. C. Martínez-García,[1,3] J. Salud,[1] M. A. Pérez-Jubindo,[2] S. Diez-Berart,[1] D. A. Dunmur,[4] and G. R. Luckhurst[4]
[1]*Grup de les Propietas Físiques dels Materials (GRPFM), Departament de Física i Enginyeria Nuclear, E.T.S.E.I.B. Universitat Politècnica de Catalunya. Diagonal, 647 08028 Barcelona, Spain*
[2]*Departamento de Física Aplicada II, Facultad de Ciencia y Tecnología, Universidad del País Vasco. Apartado 644, E-48080 Bilbao, Spain*
[3]*Department of Chemistry & Biochemistry, University of Berne, Freiestrasse 3, CH-3012 Berne, Switzerland*
[4]*School of Chemistry, University of Southampton, Southampton, SO17 1BJ, United Kingdom*

(Received 23 February 2012; accepted 20 June 2012; published online 17 July 2012)

Broadband dielectric spectroscopy spanning frequencies from 10^{-2} to 1.9×10^{9} Hz has been used to study the molecular orientational dynamics of the glass-forming liquid crystal 1″,7″-bis (4-cyanobiphenyl-4′-yl)heptane (CB7CB) over a wide temperature range of the twist-bend nematic phase. In such a mesophase two different relaxation processes have been observed, as expected theoretically, to contribute to the imaginary part of the complex dielectric permittivity. For measurements on aligned samples, the processes contribute to the dielectric response to different extents depending on the orientation of the alignment axis (parallel or perpendicular) with respect to the probing electric field direction. The low-frequency relaxation mode (denoted by μ_1) is attributed to a flip-flop motion of the dipolar groups parallel to the director. The high-frequency relaxation mode (denoted by μ_2) is associated with precessional motions of the dipolar groups about the director. The μ_1-and μ_2-modes are predominant in the parallel and perpendicular alignments, respectively. Relaxation times for both modes in the different alignments have been obtained over a wide temperature range down to near the glass transition temperature. Different analytic functions used to characterize the temperature dependence of the relaxation times of the two modes are considered. Among them, the critical-like description via the dynamic scaling model seems to give not only quite good numerical fittings, but also provides a consistent physical picture of the orientational dynamics on approaching the glass transition. © *2012 American Institute of Physics*. [http://dx.doi.org/10.1063/1.4733561]

I. INTRODUCTION

Liquid crystal dimers are a type of liquid crystal in which two semi-rigid terminal groups are linked via a flexible spacer. The terminal groups can be different or identical giving rise to two broad classes of dimers, the non-symmetric and symmetric, respectively. Initially, among the semi-rigid units, the most used were calamitic mesogens[1] though combinations of disc-like and bent-core mesogens with calamitic units, or even only bent-core units are currently being explored.[2–5] In the vast majority of systems the flexible spacers are alkyl chains, whose length and parity determine the properties and phase behavior of the materials.[6]

Liquid crystal dimers have attracted considerable attention during recent years, mainly due to new exciting findings on the fundamental level as well as possibilities for new applications such as flexoelectric-based electro-optic displays[7] due to the magnitude of the electro-optic response.[8] Novel features identified in liquid crystal dimers include alternating and modulated smectic mesophases,[5,9] the existence or not of the elusive biaxial nematic mesophase[10] and the new type of twist-bend nematic phase.[11–13] It is the behavior of this new nematic phase which forms the focus of our paper. According to predictions by Dozov[13] a negative value of the bend elastic constant can lead to a twist-bend nematics in which the director is no longer uniform but has a conical twisted and bent director distribution. It has recently been suggested by Panov *et al.*[12] that the periodic deformations in such mesophases exhibit potential applications in diffraction gratings and photonics. The possibility that the dynamic disorder of this phase could be frozen leading to a glassy state open new potential applications.

Extensive studies based on a range of techniques of the two nematic phases formed by the odd liquid crystal dimer 1″,7″-bis (4-cyanobiphenyl-4′-yl)heptane (hereafter denoted by the acronym CB7CB) have provided strong evidence that this does indeed form the twist-bend nematic phase.[11] This symmetric liquid crystal dimer has a simple molecular structure schematized as follows:

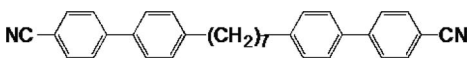

where two cyanobiphenyl groups are linked by an alkyl chain of seven methylene groups. Each mesogenic group has a dipole moment along its long axis associated with the nitrile group.

Despite the fact that the synthesis of CB7CB was reported in the 1990s,[14] little about its liquid-crystal behavior

a)Author to whom correspondence should be addressed. Electronic mail: david.orencio.lopez@upc.edu.

has been known so far. This particular dimer had been synthesized to test the prediction that the presence of methylene links linking two mesogenic groups to an odd spacer would lower the orientational order in comparison with that for the corresponding dimer with say ether links.[14] This prediction results from the greater biaxiality associated with the more bent conformers (the most energetically favored molecular shapes) and is found to be in good accord with experiment.[14] It was reported[14] that two mesophases existed below the isotropic phase (I), that at higher temperatures was identified as a nematic (N) and the other at lower temperatures was tentatively identified as a smectic A (SmA). New experimental work combining many techniques, published very recently,[11] shows that CB7CB exhibits a uniaxial nematic mesophase over the ranges ca. 390-377 K despite its bent molecular shape. At about 377 K the dimer undergoes a weakly first-order phase transition to a second disordered mesophase, devoid of long-range translational order that has been identified as another nematic mesophase. However, deuterium nuclear magnetic resonance (DNMR) measurements show that this phase must necessarily be chiral either globally or locally in domains. By combining measurements from other techniques and theoretical calculations, the study[11] concludes that this nematic mesophase is characterized by a local, probably periodic, bend in the director and is designated as a twist-bend nematic mesophase (N_{tb}). The phase appears to be relatively viscous and the viscosity seems to increase significantly on cooling, but no detailed measurements have been carried out so far. In a previous preliminary study,[15] by means of modulated differential scanning calorimetry (MDSC), it has been shown that the N_{tb} mesophase can be supercooled leading to a glass transition at about 277 K.

The main motivation of this paper is to analyze the molecular orientational dynamics of the N_{tb} mesophase formed by the polar symmetric dimer CB7CB. To do so, dielectric relaxation measurements have been performed over the entire temperature range down to close to the calorimetric glass transition. Preliminary dielectric relaxation studies[11,15] of CB7CB were interpreted using different molecular motions specified by theoretical models.[16,17] As stated,[11] in both uniaxial mesophases of CB7CB, N and N_{tb}, the dipolar moieties associated with the terminal cyanobiphenyl groups lead to two relaxation modes associated with the rotational dynamics of the molecules. The low-frequency mode, indicated by μ_1, is due to an end-over-end or flip-flop motion of the dipolar groups parallel to the director. A high-frequency mode, denoted as μ_2, is associated with precessional motions of the dipolar groups about the director. These modes contribute to the complex dielectric permittivity to different extents, depending on the alignment of the director with respect to the probing electric field.

An important part of the analysis described in this paper is devoted to the exploration of the dielectric glass transition identified in CB7CB on cooling from the twist-bend nematic phase. A glass-transition can be characterized through a temperature T_g and the rate at which various properties change with temperature on approaching the glass transition from a fluid phase. For dielectric relaxation, a glass transition, also denoted as dynamic glass transition, is defined when the associated structural relaxation time reaches 100 s, and for systems exhibiting a number of structural relaxations, it is possible to identify dielectric glass transitions corresponding to each kind of molecular motion. The results presented here for the liquid crystal dimer CB7CB are discussed to obtain information on which molecular motions are frozen on glass formation.

The structure of the paper is as follows. First, in Sec. II, a review of the functions most used to describe the temperature dependence of the dielectric relaxation time is given. In Sec. III, experimental details are provided. Our results and the procedure for data analysis are detailed in Sec. IV. Finally, a discussion of the results and concluding remarks are provided in Secs. V and VI, respectively.

II. NON-ARRHENIUS FUNCTIONS FOR THE DIELECTRIC RELAXATION TIMES

The simplest model for the dielectric absorption exhibited by many materials is that due to Debye of a simple first order rate process for the randomization of an oriented dipole. The temperature dependence of the relaxation time can then be represented by the phenomenological Arrhenius equation, which introduces an activation energy for reorientation of the molecular dipole in its dielectric environment. While the Arrhenius equation is adequate to describe the dielectric response of many simple fluids, there are numerous materials where it fails, and modified equations have been introduced to fit the experimental results. Such fitting equations are useful in the analysis of the experimental data, but the physical significance of the parameters obtained from fitting data is sometimes less than clear.

One of the phenomenological equations used most often to describe the temperature dependence of the relaxation time (τ) data is the Vogel-Fulcher-Tammann (VFT)

$$\tau = \tau_0 \exp\left[\frac{B}{T - T_0}\right], \tag{1}$$

where τ_0 is the relaxation time in the high temperature limit, B is an activation parameter and T_0 is the "ideal" glass temperature, denoted as the Vogel temperature. In fact, the VFT-equation establishes a dynamic divergence of the relaxation time at some finite temperature T_0, but there are no experimental results that conclusively prove the existence of this divergence.[18] The validity of the VFT-equation was already questioned in the 1970s[19,20] and also recently.[18,21] Despite these concerns, some theories have been based on the VFT-equation such as the Adam-Gibbs entropy model (AG),[22] Cohen-Grest (CG),[23] and some more recent theoretical models.[24,25] The underlying idea of such theories is that the glass formation is linked to highly cooperative motions in a heterogeneous (structurally fluctuating) sample, with increasing cooperativity as T_g is approached. It is proposed that a virtual phase transition exists below the glass transition temperature, which for VFT-equation is T_0.

Combining the above ideas of glass formation with a mean-field description of the virtual phase transition, the

dynamic scaling (DS) model[26,27] has been proposed such that

$$\tau = \tau_0 \left[\frac{T - T_c^{DS}}{T_c^{DS}} \right]^{-\phi}, \quad (2)$$

where the pre-factor τ_0 is defined as the relaxation time at $2T_c^{DS}$; the temperature T_c^{DS} is the temperature of the virtual phase transition (the critical temperature), usually located slightly below T_g, but no more than 20 K below; the exponent $\phi \approx 9$ was reported by Colby[26] and suggested as universal for glass-forming polymers. In spin-glass-like systems,[28] ϕ seems to range from 6 to 15 and liquid crystalline-glass systems could be considered as the *electric* analog of the *magnetic* spin-glass systems. Equation (2) seems to describe well the relaxation time data for glass-forming liquid crystals[29] in the low-temperature dynamic domain near T_g and up to the caging temperature, denoted as T_A. Such a temperature is postulated as the temperature above which all entities are moving without cooperative motions. It seems to be verified that $1.3T_c^{DS} < T_A < 1.8T_c^{DS}$.[27]

For the high-temperature dynamic domain ($T > T_A$), well above the glass transition where the coupling mechanisms can be disregarded, Mode Coupling Theory (MCT) provides a power law function similar to Eq. (2), but with fitting parameters with different physical meanings to those reported by the DS-model. The MCT critical-like equation[30] is written as

$$\tau = \tau_0 \left[\frac{T - T_c^{MCT}}{T_c^{MCT}} \right]^{-\Phi}, \quad (3)$$

where T_c^{MCT} accounts for the crossover temperature from the ergodic to the non-ergodic domain. The critical temperature T_c^{MCT} seems to correlate with the caging temperature T_A.[28] Equation (3) portrays quite well the relaxation time data of glass-forming liquid crystals for $T > T_c^{MCT} + 20\ K$ with exponents ϕ ranging from 1.5 to 4.[31]

The functions described by Eqs. (1) and (2) introduce a virtual phase transition below T_g and a dynamic divergence of the relaxation time is also required at this phase transition. Recently, some authors[18,32,33] have claimed that three-parameter non-divergent functions, without virtual phase transitions, are necessary to describe the relaxation time data over the full temperature domain. One of the most often used was the so-called Avramov equation[34] but it has been considered only to a limited extent to describe the dynamics of liquid crystalline glasses.[28,35]

An alternative non-divergent description that has recently been claimed to be superior[36] to the Avramov equation is the Waterton-Mauro (WM)-parameterization, derived empirically by Waterton[37] in the 1930s and virtually forgotten until now. After being theoretically obtained by Mauro and co-workers,[38] it is currently considered as a promising non-divergent function[33] for portraying the relaxation time, defined as follows:

$$\tau = \tau_0 \exp\left[\frac{K}{T} \exp\left(\frac{C}{T} \right) \right], \quad (4)$$

where τ_0 has the same meaning as in the VFT-equation; K and C are related with effective activation barriers, being both defined as thermal activation fitting parameters.

III. EXPERIMENTAL

The synthesis of CB7CB has been reported earlier[14] and has been synthesized accordingly. As previously stated,[11] on heating the N_{tb}-N and N-I phase transitions have been observed at 376.7 K and 389.7 K, respectively.

Measurements of the complex dielectric permittivity in the range $10^{-2}-1.9\times10^{9}$ Hz were performed using three impedance analyzers: *Agilent 4294A*, *HP 4291A*, and *Schlumberger 1260* with a *Novocontrol* dielectric interface. The cell consists of two gold-plated brass electrodes (diameter 5 mm) separated by thick silica spacers of the order of 50 μm. A modified *HP16091A* coaxial test fixture was used as the sample holder. It was held in a cryostat from *Novocontrol* and both temperature and dielectric measurements were computer-controlled. Additional details of the experimental technique can be found elsewhere.[10,11,39] Experiments were performed on cooling with different temperature steps.

Static heat capacity measurements at normal pressure were obtained using a commercial differential scanning calorimeter *DSC-Q2000* from *TA-Instruments* working in a modulated mode (MDSC). In our work, the experimental conditions (temperature amplitude and oscillation period) were adjusted to obtain only the real part (the static part) of the complex heat capacity. A more detailed description of the MDSC technique can be found elsewhere.[10,11,40] Experiments were performed on cooling from the isotropic phase down to the glassy state and on heating up to the isotropic phase, all runs made at *1* $\mathrm{K\cdot min^{-1}}$. The modulation parameters (temperature amplitude and oscillation period) were ±0.5 K and 60 s.

IV. RESULTS AND DATA ANALYSIS

A. Relaxation times

Dielectric results for CB7CB have been obtained for both the parallel and perpendicular alignments. In metallic cells the director of CB7CB spontaneously aligns parallel to the surface resulting in a perpendicular alignment of the sample with respect to the probing electric field. The fact that the dielectric anisotropy of CB7CB at low frequencies is positive[11] enables the use of a dc bias voltage (35 V equivalent to an electric field of 0.7 $\mathrm{MV\cdot m^{-1}}$) to generate parallel alignment of the director with respect to the probing electric field. Saturation of the alignment in the nematic phase was confirmed by measuring the capacitance as a function of voltage. Figures 1(a) and 1(b) show the imaginary part of the parallel and perpendicular dielectric permittivities, respectively, as functions of frequency and temperature in the isotropic phase and in both the nematic and twist-bend nematic mesophases. The dielectric relaxation results show only one mode in the isotropic phase corresponding to the concerted rotation of the whole dimer CB7CB (denoted as μ_1-mode) as expected.[11,17]

Regarding the parallel component of the permittivity, in the nematic mesophase the director is aligned parallel to the electric field because the dielectric anisotropy, $\Delta\varepsilon$, although small, is positive.[11] In the predicted conical twist-bend nematic mesophase the director is tilted with respect to the helix axis by the constant polar angle, θ_0, and the rotating

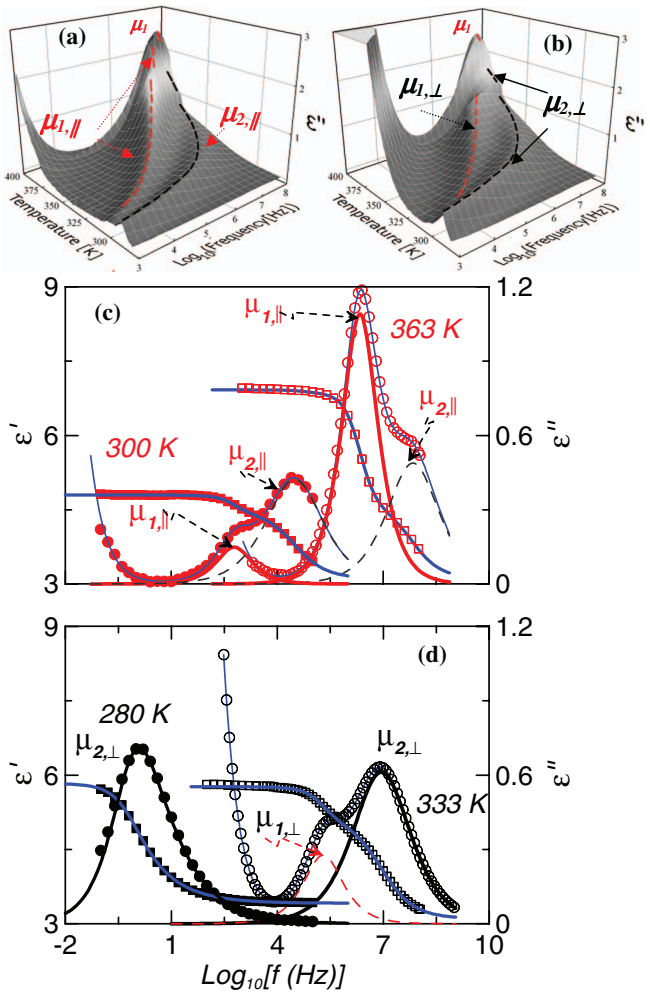

FIG. 1. Frequency and temperature dependence of the parallel component (a) and perpendicular component (b) of the permittivity (ε'' = imaginary part) of CB7CB. In the nematic mesophases (either N or N_{tb}) two relaxation modes, denoted as μ_1 and μ_2, are observed irrespective of the alignment. (c) and (d) show the parallel and the perpendicular components of the permittivity (ε' = real part and ε'' = imaginary part) at two temperatures in the N_{tb}, respectively. The circles and squares represent experimental points for ε'' and ε', respectively, while blue lines are fits to Eq. (5). Solid red and black lines correspond to the main contributing modes $\mu_{1,\parallel}$ and $\mu_{2,\perp}$, respectively. Dashed black and red lines correspond to the contributing modes $\mu_{2,\parallel}$ and $\mu_{1,\perp}$, respectively.

azimuthal angle, φ, which varies linearly with the position along the helix axis. One consequence of the Dozov prediction[13] is that since the bent molecules are achiral the system will consist of two chiral domains having opposite handedness. Provided $\Delta\varepsilon$ is positive and θ_0 is less than 54.5° then the dielectric anisotropy for these chiral domains, $\Delta\varepsilon_h$, will also be positive. Accordingly, in the nematic mesophase, the parallel component of the permittivity clearly shows two relaxations (Figure 1(a)) as predicted:[11,17] one at low-frequencies attributed to the flip-flop motions of the dipolar units (denoted as $\mu_{1,\parallel}$-mode) and another at higher frequencies due to precessional motions of the dipolar units around the director (denoted as $\mu_{2,\parallel}$-mode). The $\mu_{1,\parallel}$-mode predominates over the $\mu_{2,\parallel}$-mode, even in the low temperature nematic mesophase N_{tb} at high temperatures, as it is shown in Figure 1(c) at 363 K (open circles). As the temperature is reduced further in the N_{tb} mesophase, the amplitude of the $\mu_{1,\parallel}$-mode decreases relative to the $\mu_{2,\parallel}$-mode. This fact can be clearly shown in Figure 1(c) at 300 K (full circles), in which both modes are overlapped and the $\mu_{1,\parallel}$-mode has a smaller amplitude than $\mu_{2,\parallel}$-mode.

As for the perpendicular component of the permittivity, the high-frequency relaxation (denoted as $\mu_{2,\perp}$-mode) is dominant over the temperature range of the N-mesophase, with a very small contribution from the low-frequency relaxation ($\mu_{1,\perp}$-mode)[11] although this cannot be discerned in Figure 1(b). Conversely, at the transition to the N_{tb} mesophase, there is a sudden increase of the amplitude of the $\mu_{1,\perp}$-mode, which persists to lower temperatures, although its intensity decreases. In Figure 1(d) the relaxation spectrum of the perpendicular component (open circles) at 333 K is shown. However, at very low temperatures, at for example 280 K (full circles), the contribution of the $\mu_{1,\perp}$-mode cannot be distinguished because it is merged with the peak representative of the $\mu_{2,\perp}$-mode.

Experimental results of the complex permittivity have been analyzed using the empirical function:

$$\varepsilon(\omega) = \sum_k \frac{\Delta\varepsilon_k}{[1 + (i\omega\tau_{k,HN})^{\alpha_k}]^{\beta_k}} + \varepsilon_\infty - i\frac{\sigma_{dc}}{\omega\varepsilon_0}, \qquad (5)$$

where $\Delta\varepsilon_k$ is the dielectric strength of each relaxation mode, $\tau_{k,HN}$ is a relaxation time related to the frequency of maximum dielectric loss, α_k and β_k are parameters which describe the shape (symmetry and width) of the relaxation spectra ($\alpha_k = \beta_k = 1$ corresponds to Debye relaxation) and σ_{dc} is the dc conductivity. The summation is extended over the two relaxation modes, and each is fitted according to the Havriliak-Negami (HN) function. For the purpose of the present study we focus on the relaxation time ($\tau_{k,max}$) at the frequency of maximum dielectric loss of each relaxation mode,[28,41–44] which can be easily obtained using[45]

$$\tau_{k,\max} = \tau_{k,HN}\left[\sin\frac{\alpha_k\pi}{2+2\beta_k}\right]^{-1/\alpha_k}\left[\sin\frac{\alpha_k\beta_k\pi}{2+2\beta_k}\right]^{1/\alpha_k}, \qquad (6)$$

where $\tau_{k,HN}$, α_k, and β_k are determined from the experimental results using Eq. (5).

The $\mu_{1,\parallel}$-mode is chosen as representative of the flip-flop motions of the dipolar cyanobiphenyl units of CB7CB and the associated $[\tau_{1,max}]$ is followed over the complete temperature range down to *288* K, the lowest temperature at which an optimal analysis through Eq. (5) can be performed. The results are shown in Figure 2 and the fitted values of α_1 and β_1 through Eq. (5) are listed in Table I.

The $\mu_{2,\perp}$-mode is considered as representative of the precessional motions of the dipolar units around the local director of the CB7CB and the associated $[\tau_{2,max}]$ is followed over the entire temperature range down to 278 K. These results are shown in Figure 2 and the fitted values of α_2 and β_2 determined through Eq. (5) are listed in Table I. It should be stressed that relaxation time data corresponding to the $\mu_{1,\parallel}$-mode are not reliable below 288 K and even at about 283 K, both relaxation modes ($\mu_{1,\parallel}$-and-$\mu_{2,\parallel}$) are nearly indistinguishable.

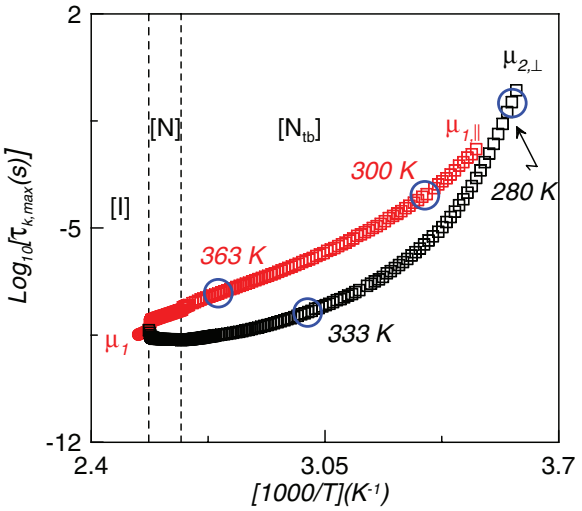

FIG. 2. Relaxation times at the frequency of maximum dielectric loss for both $\mu_{1,\parallel}$ and $\mu_{2,\perp}$ modes as a function of the inverse temperature. Blue circles indicate the representative data of 1(c) and 1(d).

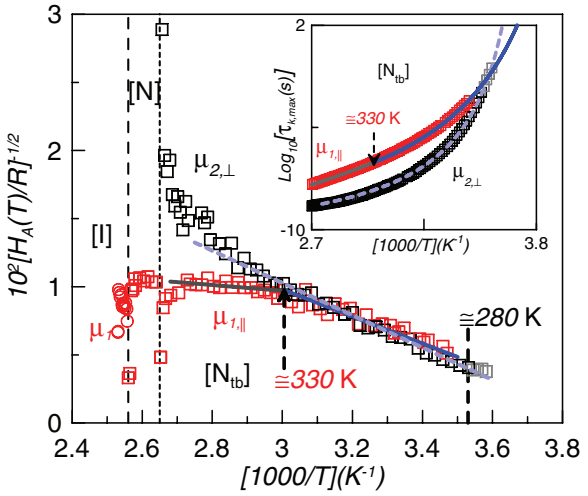

FIG. 3. Results of the temperature-derivative analysis [Eq.(7)] applied to both $\mu_{1,\parallel}$ and $\mu_{2,\perp}$ modes of CB7CB in which linear dependences indicate domains of validity of the VFT-parameterization. The inset presents the relaxation time data for both modes as an Arrhenius plot. Solid and dashed lines correspond to the dynamic domains for the $\mu_{1,\parallel}$ and $\mu_{2,\perp}$ modes, respectively, according to Eq. (7) and Eq.(1) (in the inset) with parameters taken from Table II.

B. Dynamic characterization

It has been proposed by Stickel *et al.*[41] that the temperature-derivative analysis of dynamic data (the relaxation time data in the present study) constitutes a powerful tool to obtain precise information of their variation with temperature. The main idea[28,29,35,46,47] is to proceed with derivatives of very accurate $ln[\tau_{k,max}]$ data with respect to temperature to test the validity of the parameterizations determined from Eq. (1) to Eq. (4).

By applying the temperature-derivative procedure proposed by Drozd-Rzoska and Rzoska[46] to Eq. (1), we find

$$\left[\frac{d\ln\tau}{d(1/T)}\right]^{1/2} = \left[\frac{H_A(T)}{R}\right]^{-1/2} = B^{-1/2}\left(1-\frac{T_0}{T}\right), \tag{7}$$

where $H_A(T)$ is denoted as the *apparent activation enthalpy*.[46] In the region of validity of the VFT-equation, Eq. (7) predicts a linear dependence of the $[H_A(T)/R]^{-1/2}$ on inverse temperature.

The application of Eq. (7) to both $\mu_{1,\parallel}$ and $\mu_{2,\perp}$ modes of CB7CB is presented in Figure 3. Focusing on the N_{tb} mesophase at temperatures well below the N-N_{tb} phase transition it can be observed that the activation enthalpies associated with both modes merge at about 330 K and apparently follow the same trend as the temperature decreases. In addition, this temperature seems to be either coincident or close to the dynamic crossover exhibited by the $\mu_{1,\parallel}$-data. At temperatures above this dynamic crossover, the dynamics of $\mu_{1,\parallel}$-mode is more Arrhenius-like. The dynamics of $\mu_{2,\perp}$-mode becomes more Arrhenius-like when temperature approaches glass transition, a fact already observed in other materials.[21] Such data, according to Figure 3, seem to follow a linear dependence from low temperatures (about 280 K) up to about 360 K (about 2.8 K^{-1} scaled as 1000/T). Lines (dashed and solid) in Figure 3 represent linear fits according to Eq. (7) for the different dynamic domains. The VFT-parameters, after refining through Eq. (1) to obtain the pre-factor τ_0, are listed in Table II where the dynamic domains are identified. The inset in Figure 3 shows the relaxation time data for both modes in an Arrhenius plot, but only in the temperature range of the N_{tb}-mesophase. Solid and dashed lines show VFT-fittings with parameters taken from Table II.

It should be stressed as can be observed in the inset of Figure 3 and more precisely in Table II, that two different dielectric glass transition temperatures are obtained, though rather close one to another within about 5 K. It is also interesting to note that the pre-factor τ_0 for the $\mu_{2,\perp}$-mode is of the order of 10^{-11} s.

We now consider the temperature-derivative procedure to be applied to the critical-like description through

TABLE I. Fitting parameters (α and β) according to Eq. (5) for the $\mu_{1,\parallel}$-and- $\mu_{2,\perp}$-modes.

	$\mu_{1,\parallel}$-mode			$\mu_{2,\perp}$-mode		
Phase	α_1	β_1	Temperature range	α_2	β_2	Temperature range
N	0.92	1.0	All range of existence	0.70	1.0	All range of existence
N_{tb}	0.97	1.0	377 K-288 K	0.67	1.0	377 K-318 K
				$\alpha_2 \cdot \beta_2$		
				0.65-0.47[a]		318 K-278 K

[a]The value decreases monotonically as temperature decreases.

TABLE II. Fitting parameters according to Eq. (1) for the different dynamic domains and the calculated glass transition temperature for the $\mu_{1,\parallel}$-and-$\mu_{2,\perp}$-modes.

Mode	$\log_{10}[\tau_0(s)]$	B(K)	T_0(K)	T_{gl}(K)	Range[1000/T(K^{-1})]
$\mu_{1,\parallel}$	−13.15	2702	168.1	…	2.7–3
	−10.25	928.5	237.0	269.8	3–3.5
$\mu_{2,\perp}$	−10.45	474.9	259.1	275.2	≈2.8-(≈3.6)[a]

[a]Dynamic crossover at about 280 K has not been taken into account.

TABLE III. Fitting parameters according to Eqs. (2) and (3) for the different dynamic domains and the calculated glass transition temperature for the $\mu_{1,\parallel}$ and $\mu_{2,\perp}$-modes.

Mode	$log_{10}[\tau_0(s)]$	$T_C^X(K)$	ϕ	$T_{gl}(K)$	Range[1000/$T(K^{-1})$]	Description
$\mu_{1,\parallel}$	−10.07	273.1	6.2	275.8	2.7–3.5	DS
$\mu_{2,\perp}$	−9.822	318.0	1.6	…	2.7–3	MCT
	−12.87	273.5	7.4	276.2	3-(≈3.6)	DS

Eqs. (2) and (3). A linear dependence with temperature is obtained in the region of validity of the critical-like descriptions according to the relationship:

$$T^2\left[\frac{d\ln\tau}{d(1/T)}\right]^{-1} = \left[\frac{T^2R}{H_A(T)}\right] = \frac{1}{\Phi}\left(T - T_C^X\right), \qquad (8)$$

where T_C^X accounts for either T_C^{DS} in the DS-model (Eq. (2) and $T_C^{DS}<T_g$) or T_C^{MCT} in the MCT-description (Eq. (3) and $T_C^{MCT} \gg T_g$). Details for the derivation of Eq. (8) have been given by Drozd-Rzoska and Rzoska.[46]

Experimental data for both modes of CB7CB are shown in Figure 4 as a plot of $[T^2R/H_A(T)]$ vs. temperature. It should be stressed that the $\mu_{1,\parallel}$-data exhibit a linear behavior (i.e., follow the DS-model) over the entire temperature range of the N_{tb}-mesophase, from low to high temperatures and even in the N mesophase. However, $\mu_{2,\perp}$-data in the N_{tb}-mesophase clearly show two linear domains, one at low temperatures (DS-model) from T_g up to about 330 K (denoted as T_A in the figure) and another at high temperatures (MCT description) from T_A up to the vicinity of the N_{tb}-N phase transition. In addition, the results for both modes seem to be indistinguishable from low temperatures to about T_A. The subsequent linear fittings according to Eq. (8) yield the values of the parameters for each mode and dynamic domain, namely T_C^{DS}, T_C^{MCT} and the exponent ϕ. The final fitting of the relaxation data according to either Eq. (2) or Eq. (3) is focused on the pre-factor τ_0. All these refined parameters are listed in Table III and results of the fittings are drawn on Figure 4 and on the inset where the relaxation time data are presented as an Arrhenius plot.

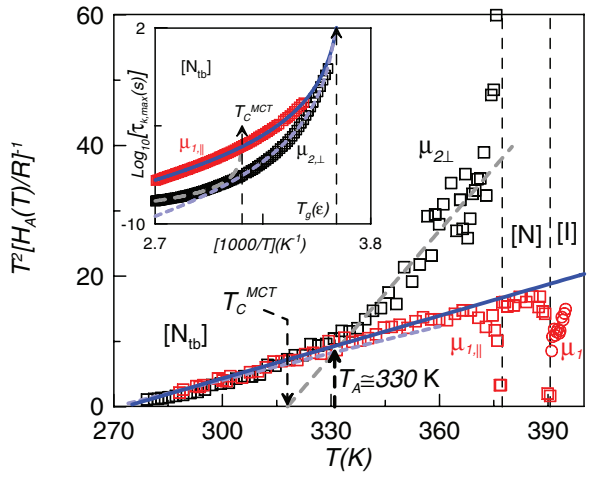

FIG. 4. Results of the temperature-derivative analysis [see Eq. (8)] applied to both $\mu_{1,\parallel}$ and $\mu_{2,\perp}$ modes of CB7CB in which linear dependences indicate domains of validity of the critical-like description. The inset presents the relaxation time data for both modes as an Arrhenius plot. Solid and dashed lines correspond to the dynamic domains for $\mu_{1,\parallel}$ and $\mu_{2,\perp}$ modes, respectively, according to Eq. (8) and Eqs. (2) and (3) (in the inset) calculated with parameters taken from Table III.

One of the most noticeable results in Table III is related to both the $T_C^{DS}$and T_g temperatures corresponding to the $\mu_{1,\parallel}$-and-$\mu_{2,\perp}$-modes. It seems that a common critical temperature (≈273 K) for the virtual phase transition and also the same glass transition temperature of about 276 K are obtained for both modes. As for the exponent, in the DS-domain, ϕ is 6.2 ($\mu_{1,\parallel}$-mode) and 7.4 ($\mu_{2,\perp}$-mode), typical values usually reported for spin-glass-like systems.[28] In the MCT-domain for the $\mu_{2,\perp}$-mode, ϕ is within the usual range of values.[31] It is also found that T_A is about $1.04T_C^{MCT}$, a value not too far from that found in other glass-forming liquid crystals.[28]

The application of the temperature-derivative procedure to Eq. (4) does not allow a similar straightforward linearization methodology as followed in Eqs. (7) and (8). Instead an enthalpy function is obtained with two uncorrelated linear variables (K and C) in the form:

$$\frac{d\ln\tau}{d(1/T)} = \frac{H_A(T)}{R} = K\left(1 + \frac{C}{T}\right)e^{C/T}. \qquad (9)$$

As suggested recently,[36,48] to proceed further with a successfully linearized expression, Eq. (9) can be written as:

$$\ln\left[\frac{H_A(T)}{R(1+(C/T))}\right] = Ln(K) + \frac{C}{T}. \qquad (10)$$

The procedure for fitting the relaxation time data of both modes of CB7CB to Eq. (10) consists of a minimization approach[48] of the 3D-weighted square residuals surface merit function $\chi^2_{HA-3D} = f(C, K)$ associated with the 3D-enthalpy space[36]

$$\chi^2_{HA-3D}(C,K) = \frac{1}{N-2}\sum_{i=1}^{N}\left(1 - \frac{H_{A,i}(T_i)}{RK(1+(C/T_i))e^{C/T_i}}\right)^2. \qquad (11)$$

The summation is extended over the number N of τ-data. The minimization procedure embodied in Eq. (11) provides an easier and more accurate numerical solution than that found by direct fitting to Eq. (4). It allows us to obtain K and C parameters and, consequently, the glass transition temperatures for both relaxation modes. It should be mentioned that Eq. (11) has been successfully used for other more complex

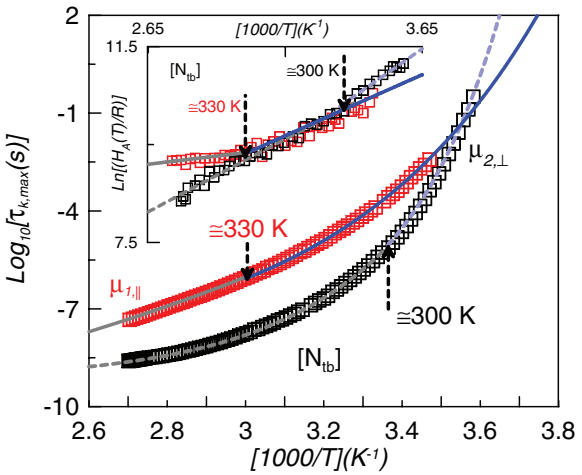

FIG. 5. Dielectric relaxation time for both $\mu_{1,\parallel}$ and $\mu_{2,\perp}$ modes in the N_{tb}-mesophase of CB7CB as a function of temperature presented in the form of an Arrhenius plot showing regions of the validity of Eq. (4). The inset shows the results of the temperature-derivative analysis that, according to Eq. (9) and the parameters listed in Table IV, should exhibit nearly linear dependences for each dynamic domain. Solid and dashed lines correspond to the dynamic domains for the $\mu_{1,\parallel}$ and $\mu_{2,\perp}$ modes, respectively.

problems as in the case of the secondary relaxation processes in orientationally disorderd crystals.[48]

The fitting procedure followed is unable to fit to only one dynamic domain for each mode as observed in Figure 5. The inset of Figure 5, in which $ln[H_A(T)/R]$ vs.$(1000/T)$ is plotted, allows us to better distinguish the different dynamic domains. It should be stressed that according to Eq. (9) and the results of the fits for the C and K parameters (see Table IV), $ln[H_A(T)/R]$ exhibits a nearly linear dependence with the inverse of temperature. Different crossover temperatures for each set of relaxation modes, one at about 300 K for $\mu_{2,\perp}$-data and another at about 330 K for $\mu_{1,\parallel}$-data, can be observed. The former has not been appreciated for VFT or critical-like analyses of $\mu_{2,\perp}$-data. However, the latter has already been observed in the VFT analysis of $\mu_{1,\parallel}$-data and apparently coincides with the estimation of the caging temperature, T_A, shown by the $\mu_{2,\perp}$-data.

The final fitting of the relaxation time data according to Eq. (4) leads to the pre-factor τ_0. All the (WM)-fitting parameters C, K, and τ_0, for each dynamic domain and relaxation mode, are listed in Table IV. The final fits are also drawn in Figure 5.

If we focus on the results for τ_0 and T_g (see Table IV), a strong parallelism with the VFT-results can be observed. Again, τ_0 for the $\mu_{2,\perp}$-mode is of the order of 10^{-11} s (high temperature dynamic domain), far from 10^{-14} s. As for the glass transition temperature, two different values are obtained, ca. 7 K apart.

TABLE IV. Fitting parameters of Eq. (4) for the different dynamic domains and the calculated glass transition temperature for the $\mu_{1,\parallel}$-and- $\mu_{2,\perp}$-modes.

Mode	$\log_{10}[\tau_0(s)]$	K(K)	C(K)	T_{gl}(K)	Range[1000/T(K^{-1})]
$\mu_{1,\parallel}$	−12.03	1162	459.3	—	2.7–3
	−8.381	10.27	1717	267.0	3–3.5
$\mu_{2,\perp}$	−9.186	0.036	2667	—	2.7-(≈3.37)
	−8.453	0.011	3642	274.1	≈3.37-(≈3.6)

V. DISCUSSION

A. Glass transition temperature and cooperative motions

The glass-forming liquid crystal dimer CB7CB exhibits two dielectric relaxation modes, and so an important question is whether the same dielectric glass transition temperature is observed for both modes ($\mu_{1,\parallel}$ and $\mu_{2,\perp}$) or if two different glass transition temperatures are detected. One of the most striking results from the detailed analysis presented in this paper is that among the analyzed dynamic parameterizations, only the critical-like description leads to a single glass transition temperature.

Let us consider the dielectric glass transition temperature associated with the $\mu_{2,\perp}$-mode: T_g ranges from 274.1 K (WM equation) to 276.2 K (DS-model), passing through 275.2 K for the VFT-equation. Different dynamic crossover temperatures are observed depending on the parameterizations, with the exception of the VFT-equation for which the fitting was made over the widest dynamic domain because the crossover was not taken into account. However, it is important to realize that the value of the pre-factor $\tau_0 \approx 10^{-11}$ s (see Table II; the value should be of the order of 10^{-14} s) represents a serious concern in the VFT-description of such a mode. From this, we consider that the preferred model is the critical-like description, although we are aware that all parameterizations provide nearly the same result for the dielectric glass transition temperature.

We now consider the dielectric glass transition temperature corresponding to the $\mu_{1,\parallel}$ -mode. With the exception of the critical-like description for which the full temperature range is well described by the DS-model with a glass transition temperature of 275.9 K, the other parameterizations exhibit a dynamic crossover at about 330 K. In this case, the low temperature dynamic domain leads to a glass transition of 269.8 K (VFT-equation) or 267.0 K (WM equation), the latter is nearly 10 K lower than that of the DS-model. In our opinion, the lack of relaxation time data for the $\mu_{1,\parallel}$ -mode below 288 K may be responsible for such a difference.

Figure 6 shows the heat capacity of CB7CB on heating and on cooling over a wide temperature range. The glass transition is clearly seen in the figure and with more detail in the inset in which both the jump in the heat capacity and the peak in the MDSC-phase shift angle (ϕ, the phase lag between the modulated temperature rate and the modulated heat flow) are shown. The maximum in the phase shift angle at the given period is assigned to the dynamic glass transition temperature.[44] Such results argue unambiguously for a single dynamic glass transition occurring at a temperature of about 277 K. Among the different dynamic parameterizations used to fit the dynamic data, only the critical-like description via the DS-model in the ultraviscous domain predicts a single glass transition temperature at about 276 K (see Table II), very close to 277 K, for both molecular modes ($\mu_{1,\parallel}$ and $\mu_{2,\perp}$).

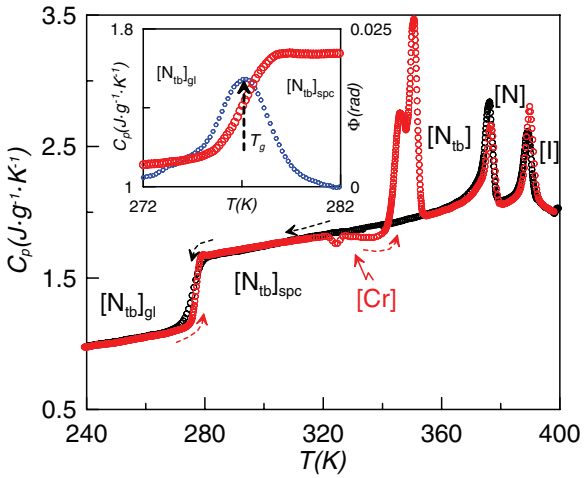

FIG. 6. Heat capacity measurements for CB7CB on slow cooling (black symbols) and slow heating (red symbols). The inset shows, in detail, the jump in the heat capacity (red symbols) as well as the peak in the ϕ-shift angle (blue symbols) as a signature of the glass transition experienced by the twist-bend nematic mesophase. The crystal phase only appears on heating the supercooled twist-bend nematic mesophase.

Considering the information contained in Figure 4, molecular motions associated with the $\mu_{1,\parallel}$-mode, i.e., flip-flop motions of the rigid mesogenic units of the dimer, can be well-described by the DS-model over the full temperature range of the N_{tb} mesophase. According to the DS-model, these molecular motions should be highly cooperative or strongly correlated over the range of existence of the mesophase, that is to say, they do not seem to have sufficient free volume to be produced without cooperativity at any temperature.

The nematic liquid crystal phases formed by the dimer CB7CB should be regarded as a mixture of many conformers. Calculations[11] using the continuous torsional potential lead to a distribution of conformers with two preponderant configurations but with a wide distribution. These are identified as molecular hairpins with angles between the two rigid cores of about 30° and those considered as extended V molecular shapes with angles between the mesogenic groups of around 120°. At higher values of the order parameter (lower values of temperature) the extended V molecular shapes are stabilized at the expense of the less extended conformers (hairpin). In the nematic mesophases, either N or N_{tb}, the population of the extended conformers compared with the less extended (hairpin) ones is dominant at any temperature, and increases even more as the temperature decreases. Cooperativity is said to be favored by a strongly anisotropic environment[49] that for flip-flop motions seem to be enough at any temperature in the nematic mesophases, either N or N_{tb}.

For the $\mu_{2,\perp}$-mode shown in Figure 4, it is observed that the DS-model is verified from low temperature up to T_A of about 330 K ($\approx 1.25T_C$). In this temperature range, precessional motions of the dipolar groups about the local director should be strongly coupled, the activation enthalpies being similar to that of the flip-flop motions ($\mu_{1,\parallel}$-mode). Probably, the coupling in both molecular motions is due to the strongly anisotropic environment[49] as we have suggested above. But for precessional motions, on increasing temperature up to about T_A, the anisotropy caused by the population of the extended conformers seems not to be enough and a decoupling phenomenon is observed. However, coupling of flip-flop motions remains and molecules never have sufficient free volume to become decoupled.

A coherent physical picture of flip-flop dipolar dynamics in the nematic phase of liquid crystal dimers was proposed by Stocchero *et al.*[17] who formulated a theoretical model based on a simplified nematic potential that exhibits four-deep wells (the so-called four-state model). The model only considers the flip-flop motion of the dipolar end groups, and any dynamic processes associated with the motion of the connecting, flexible, methylene chain are neglected. The justification for this, at least in the nematic mesophases of CB7CB, is that relaxations associated with the flip-flop mode ($\mu_{1,\parallel}$) and the precessional mode ($\mu_{2,\perp}$) occur at very different frequencies: consequently a time-scale separation can be assumed. The structural feature of the dipolar groups of CB7CB is that there is a dipole moment along the axis of the mesogenic group, and it is the rotational dynamics of this dipole in its environment, liquid crystalline or glass-like, which determines the strengths and frequencies of any dielectric relaxation. Considering a single group dipole in its environment requires two angles, polar and azimuthal, to specify its orientation. Thus it is reasonable to suggest that there can be two relaxation modes associated with these: precessional (azimuthal angle) and flip-flop (polar angle). However in an ordered environment which becomes increasingly viscous, it is likely that the modes will become mixed, i.e., they are no longer normal modes. Furthermore, the frequencies of the two modes will become closer as the dipolar groups interact more strongly with their environment. This is what is observed experimentally, and this supports strongly the proposal that there is only a single glass transition temperature. Our interest in the glass-forming properties of CB7CB has so far focused on a microscopic approach to the rotational dynamics of the molecules. An alternative perspective is to identify macroscopic features of the properties of glass-forming materials which may correlate with the physical processes necessary for the formation of the glassy-state. One such feature is the so-called "fragility" of fluids and how it might relate to the ability for form a glass.

B. Fragility

The fragility concept[50] emerged to account for the manner in which the dynamic properties of the glass forming materials change as long as the glass transition temperature is approached. One of the formalisms most used to quantify the fragility concept is the so-called *m*-fragility or steepness index[51] defined by the slope at T_g for a plot of $log_{10}(\tau)$ vs. T_g/T (known as Angell's plot). The minimum physically reliable value of *m* is considered to be 16 (estimated from a VFT-equation with $\tau_0 = 10^{-14}$ s)[51] for the strongest glass-forming material and the value of *m* increases with the fragility.

Initially, the fragility concept was applied to structural glass-forming materials in which the liquid state can vitrify. It was usual to associate the fragility concept to the material but

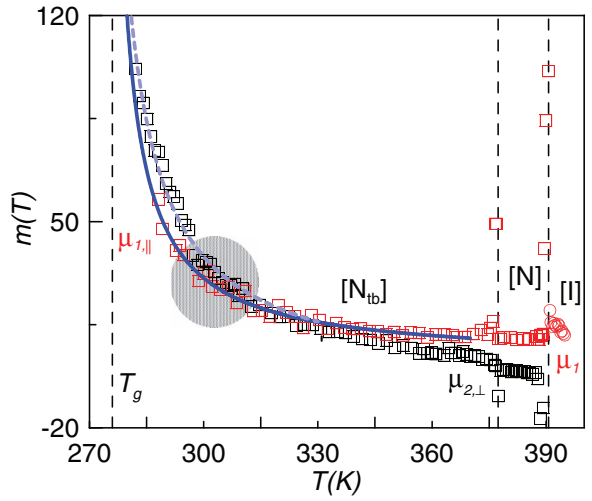

FIG. 7. Results for the temperature dependent steepness index $m(T)$ (see Eq. (12)) for the $\mu_{1,\parallel}$ and $\mu_{2,\perp}$ modes of CB7CB. Solid ($\mu_{1,\parallel}$ mode) and dashed ($\mu_{2,\perp}$ mode) lines correspond to the $m(T)$ functions according to the DS-model using the parameters given in Table III. The shadow region corresponds to the change in the trend of the $m(T)$-data as the temperature decreases.

there are materials that exhibit several dynamically disordered phases which can alternately vitrify.[39,52] In such cases, the fragility concept was associated with every disordered phase that becomes a glassy state, and so, a material can have different values of m. The N_{tb} mesophase of the liquid crystal dimer CB7CB exhibits two different kinds of molecular motions with their corresponding dynamic regimes that seem to freeze at the same T_g giving rise to the glassy N_{tb}-state. In this case, how could the fragility of the nematic mesophase that vitrifies be defined? At first glance (see Figure 2), it seems that two different values of m, one for each relaxation mode, should be obtained. To clarify this puzzle, it is convenient to define the temperature dependent steepness index $m(T)$ (Ref. 46) as

$$m(T) = \frac{H_A(T)}{R}\frac{\log_{10} e}{T}. \tag{12}$$

Substitution of $T = T_g$ in Eq. (12) yields the m-fragility defined by Angell *et al.* Equation (12) has the advantage of providing information about the dynamics not only at T_g but also as long as the material approaches the glass transition.

Figure 7 shows the temperature dependence of $m(T)$ for both relaxation modes $\mu_{1,\parallel}$ and $\mu_{2,\perp}$ of CB7CB. It is observed that the steepness index of both modes experience the same sudden but continuous increase as the temperature decreases (see the shadow region of Figure 7). Despite the apparent abrupt change, the DS-model follows quite well the evolution of both steepness indices and for the $\mu_{1,\parallel}$-mode, over the complete temperature range of the N_{tb} mesophase. Solid and dashed blue lines have been drawn according to the DS-model (Eq. (2)) using the parameters given in Table III.

The question now is: what happens just at the glass transition temperature? Or to be more precise: would the value of $m(T)$ be unique at T_g? We think that at a low enough temperature, both motions represented by $\mu_{1,\parallel}$ and $\mu_{2,\perp}$ are in a strongly cooperative dynamic regime changing in a coordinated fashion when the material approaches its glass transition temperature. Consequently, a unique value of $m(T)$ at T_g should be obtained. However, it should be stressed that the value of $m(T_g)$ obtained is very dependent on the dynamic description used. In addition, as reflected in Figure 7, the value of $m(T)$ according to the DS-model tends asymptotically to infinity at the critical temperature which, in our case, is very close to T_g leading to a relatively high value of $m(T_g)$. The value of $m(T)$ according to the VFT-equation also tends asymptotically to infinity, but at T_0 (nearly 30 K different from T_g, see Table II).

Finally, it should be mentioned that we only know of one case, reported by Brás *et al.*,[44] where two different kinds of molecular motions with their corresponding dynamic regimes were studied on approaching the glass transition. In such a study, it was concluded that only one of these molecular motions, *the dielectric tumbling mode [. . .] is responsible for glassy dynamics in the nematic liquid crystal E7* (liquid crystal mixture). While this might be true for monomeric liquid crystals, in the dimer CB7CB, results for which are reported in this paper, the so-called dielectric tumbling mode of the dipolar end groups can be coupled to the precessional mode through the flexible methylene linking chain. As the glass transition is approached, the flexibility of the methylene chain is reduced to the extent that the precessional and flip-flop modes become indistinguishable. At least that seems to be the evidence of the experiments.

VI. CONCLUDING REMARKS

Recent studies of CB7CB (Ref. 11) have shown it to be a remarkable liquid crystalline material because of the existence of an unconventional N-mesophase (the twist-bend nematic-N_{tb}) characterized by a local, probably periodic, bend in the director. However, we now know that the material is also remarkable for the glassy behavior of the N_{tb}-mesophase. The two different molecular motions detected for the glassy dynamics of the mesophase appear to behave differently from other calamitic nematics.[44] The question now is: how unusual is the glassy behavior of the CB7CB liquid crystal dimer? Or to be more precise: what should be expected for ordinary conventional glass-forming nematic liquid crystal?

The critical-like description linked to dynamic domains with cooperative motions is quite adequate to describe properly the dynamic regime associated with the two main molecular motions in the N_{tb}-mesophase of CB7CB. Both kinds of molecular motion seem to be strongly cooperative at low temperatures changing in a coordinated fashion as the material approaches its glass transition temperature. As a consequence, both molecular motions are considered to be responsible for the glassy dynamics with only one glass transition temperature and with only one value of the steepness index m at T_g, as expected. The fact that the critical-like description represents a model in which the relaxation time diverges at a temperature (T_C) very close to the glass transition temperature gives rise to a high value of the steepness index $m(T_g)$.

ACKNOWLEDGMENTS

The authors are grateful for financial support from the MICINN project MAT2009-14636-C03-02,03 and from the Gobierno Vasco (GI/IT-449-10). The authors also thank the recognition from the Generalitat de Catalunya of GRPFM as an Emergent Research Group (2009-SGR-1243). N. Sebastián would like to thank the Universidad del País Vasco for a pre-doctoral grant.

[1] C. T. Imrie and G. R. Luckhurst, "Liquid crystal dimers and oligomers," in *Handbook of Liquid Crystals Vol. 2B: Low Molecular Weight Liquid Crystals*, edited by D. Demus, J. W. Goodby, G. W. Gray, H. W. Spiess, and V. Vill (Wiley-VCH, Weinheim, Germany, 1998), Chap. X, p. 801.
[2] C. V. Yelamaggad, S. K. Prasad, G. G. Nair, I. S. Shashikala, D. S. S. Rao, C. V. Lobo, and S. Chandrasekhar, Angew. Chem., Int. Ed. **43**, 3429 (2004).
[3] M. G. Tamba, B. Kosata, K. Pelz, S. Diele, G. Pelzl, Z. Vakhovskaya, H. Kresse, and W. Weissflog, Soft Matter **2**, 60 (2006).
[4] S. Umadevi and B. K. Sadashiva, Liq. Cryst. **34**, 673 (2007).
[5] C. T. Imrie and P. A. Henderson, Chem. Soc. Rev. **36**, 2096 (2007).
[6] G. R. Luckhurst, in *Recent Advances in Liquid Crystalline Polymers*, edited by L. Lawrence Chapoy (Elsevier Applied Science, Barking, UK, 1985), Chap. 7, p. 105; A. Ferrarini, G. R. Luckhurst, P. L. Nordio, and S. J. Roskilly, J. Chem. Phys. **100**, 1460 (1994); G. R. Luckhurst and S. Romano, J. Chem. Phys. **107**, 2557 (1997).
[7] J. S. Patel and Sin-Doo Lee, J. Appl. Phys. **66**, 1879 (1989).
[8] S. M. Morris, M. J. Clarke, A. E. Blatch, and H. J. Coles, Phys. Rev. E **75**, 041701 (2007).
[9] M. S. Sepelj, U. Baumeister, S. Diele, H. L. Nguyen, and D. W. Bruce, J. Mat. Chem. **17**, 1154 (2007).
[10] N. Sebastian, M. R. de la Fuente, D. O. López, M. A. Pérez-Jubindo, J. Salud, S. Diez-Berart, and M. B. Ros, J. Phys. Chem. B **115**, 9766 (2011); N. Sebastian, D. O. López, S. Diez-Berart, M. R. de la Fuente, J. Salud, M. A. Pérez-Jubindo, and M. B. Ros, Materials **4**, 1632 (2011).
[11] M. Cestari, S. Diez-Berart, D. A. Dunmur, A. Ferrarini, M. R. de la Fuente, D. J. B. Jackson, D. O. López, G. R. Luckhurst, M. A. Pérez-Jubindo, R. M. Richardson, J. Salud, B. A. Timimi, and H. Zimmermann, Phys. Rev. E **84**, 031704 (2011).
[12] V. P. Panov, M. Nagaraj, J. K. Vij, Y. P. Panarin, A. Hohlmeier, M. G. Tamba, R. A. Lewis, and G. H. Mehl, Phys. Rev. Lett. **105**, 167801 (2010).
[13] I. Dozov, Europhys. Lett. **56**, 247 (2001).
[14] P. J. Barnes, A. G. Douglass, S. K. Heeks, and G. R. Luckhurst, Liq. Cryst. **13**, 603 (1993).
[15] S. Diez-Berart, N. Sebastian, D. O. López, M. A. Pérez-Jubindo, M. R. de la Fuente, J. Salud, and D. A. Dunmur, *23th International Liquid Crystal Conference*, Kraków (Poland), July 11–16, 2010, Abstract P3.5.
[16] P. L. Nordio, G. Rigatti, and U. Segre, Mol. Phys. **25**, 129 (1973).
[17] M. Stocchero, A. Ferrarini, G. J. Moro, D. A. Dunmur, and G. R. Luckhurst, J. Chem. Phys. **121**, 8079 (2004).
[18] T. Hecksher, A. B. Nielsen, N. B. Olsen, and J. C. Dyre, Nat. Phys. **4**, 737 (2008).
[19] W. T. Laughlin and D. R. Uhlman, J. Phys. Chem. **76**, 2317 (1972).
[20] S. M. Breitling and J. H. Magill, J. Appl. Phys. **45**, 4167 (1974).
[21] G. B. McKenna, Nat. Phys. **4**, 673 (2008).
[22] G. Adams and J. H. Gibbs, J. Chem. Phys. **43**, 139 (1965).
[23] M. H. Cohen and G. S. Grest, Phys. Rev. B **20**, 1077 (1979).
[24] J. P. Bouchaud and G. Biroli, J. Chem. Phys. **121**, 7347 (2004).
[25] V. Lubchenko and P. G. Wolynes, Ann. Rev. Phys. Chem. **58**, 235 (2007).
[26] R. H. Colby, Phys. Rev. E **61**, 1783 (2000).
[27] B. M. Erwin and R. H. Colby, J Non-Cryst. Solids **307–310**, 225 (2002).
[28] A. Drozd-Rzoska, S. J. Rzoska, S. Pawlus, J. C. Martínez-García, and J. Ll. Tamarit, Phys. Rev. E **82**, 031501 (2010).
[29] A. Drozd-Rzoska, S. J. Rzoska, and M. Paluch, J. Chem. Phys. **129**, 184509 (2008).
[30] W. Götze and L. Sjögren, Rep. Prog. Phys. **55**, 241 (1992); E. Donth, *The Glass Transition: Relaxation Dynamics in Liquids and Disordered Material*, Springer Series in Material Science II, Vol. 48 (Springer-Verlag, Berlin, 1998).
[31] *Broadband Dielectric Spectroscopy*, edited by F. Kremer and A. Schönhals (Springer-Verlag, Berlin, 2003).
[32] Y. S. Elmated, D. Chandler, and J. P. Garrahan, J. Phys. Chem. B **113**, 5563 (2009).
[33] P. Lunkenheimer, S. Kastner, M. Köhler, and A. Loidl, Phys. Rev. E **81**, 051504 (2010).
[34] T. A. Litovitz, J. Chem. Phys. **20**, 1088 (1952); A. J. Barlow, J. Lamb, and A. J. Matheson, Proc. R. Soc. London, Ser. A **292**, 322 (1966); H. Bässler, Phys. Rev. Lett. **58**, 767 (1987); I. Avramov, J. Non-Cryst. Solids **351**, 3163 (2005).
[35] A. Drozd-Rzoska, J. Chem. Phys. **130**, 234910 (2009).
[36] J. C. Martínez-García, J. Ll. Tamarit, and S. J. Rzoska, J. Chem. Phys. **134**, 024512 (2011).
[37] S. C. Waterton, J. Soc. Glass. Technol. **16**, 244 (1932).
[38] J. C. Mauro, Y. Yue, A. J. Ellison, P. K. Gupta, and D. C. Allan, Proc. Natl. Acad. Sci. U.S.A. **106**, 19780 (2009).
[39] R. Puertas, M. A. Rute, J. Salud, D. O. López, S. Diez, J. C. Van Miltenburg, L. C. Pardo, J. Ll. Tamarit, M. Barrio, M. A. Pérez-Jubindo *et al.*, Phys. Rev. B **69**, 224202 (2004).
[40] M. B. Sied, J. Salud, D. O. López, M. Barrio, and J. Ll. Tamarit, Phys. Chem. Chem. Phys. **4**, 2587 (2002).
[41] F. Stickel, E. W. Fischer, and R. Richert, J. Chem. Phys. **102**, 6251 (1995).
[42] R. Richert and C. A. Angell, J. Chem. Phys. **108**, 9016 (1998).
[43] M. Tyagi and S. S. N. Murthy, J. Chem. Phys. **114**, 3640 (2001).
[44] A. R. Brás, M. Dionísio, H. Huth, Ch. Schick, and A. Schönhals, Phys. Rev. E **75**, 061708 (2007).
[45] R. Richert, F. Stickel, R. S. Fee, and M. Maroncelli, Chem. Phys. Lett. **229**, 302 (1994).
[46] A. Drozd-Rzoska and S. J. Rzoska, Phys. Rev. E **73**, 041502 (2006).
[47] S. Pawlus, M. Paluch, M. Sekula, K. L. Ngai, S. J. Rzoska, and J. Ziolo, Phys. Rev. E **68**, 021503 (2003); S. Pawlus, R. Casalini, C. M. Roland, M. Paluch, S. J. Rzoska, and J. Ziolo, Phys. Rev. E **70**, 061501 (2004).
[48] J. C. Martínez-Garcia, Ph.D. thesis, Technical University of Catalonia, Barcelona, 2011.
[49] L. de Gaetani, G. Prampolini, and A. Tani, J. Chem. Phys. **128**, 194501 (2008).
[50] C. A. Angell, in *Relaxations in Complex Systems*, edited by K. Ngai and G. B. Wright (Springfield, 1985); C. A. Angell, J. Phys. Chem. Solids **49**, 863 (1988); C. A. Angell, J. Non-Cryst. Solids **131–133**, 13 (1991).
[51] R. Böhmer and C. A. Angell, Phys. Rev. B **45**, 10091 (1992); R. Böhmer, K. L. Ngai, C. A. Angell, and D. J. Plazek, J. Chem. Phys. **99**, 4201 (1993).
[52] R. Puertas, J. Salud, D. O. López, M. A. Rute, S. Diez, J. Ll. Tamarit, M. Barrio, M. A. Pérez-Jubindo, M. R. de la Fuente, and L. C. Pardo, Chem. Phys. Lett. **401**, 368 (2005).